Mapping landscape friction to locate isolated tsetse populations that are candidates for elimination

Jérémy Bouyer[a,b,c,d,1], Ahmadou H. Dicko[e], Giuliano Cecchi[f], Sophie Ravel[g], Laure Guerrini[h,i], Philippe Solano[g], Marc J. B. Vreysen[j], Thierry De Meeûs[g,k], and Renaud Lancelot[a,b]

[a]Centre de Coopération Internationale en Recherche Agronomique pour le Développement, Unité Mixte de Recherche Contrôle des Maladies Animales Exotiques et Emergentes, Campus International de Baillarguet, 34398 Montpellier, France; [b]Institut National de la Recherche Agronomique, Unité Mixte de Recherche 1309 Contrôle des Maladies Animales Exotiques et Emergentes, 34398 Montpellier, France; [c]Centre de Coopération Internationale en Recherche Agronomique pour le Développement, Unité Mixte de Recherche Interactions Hôtes-Vecteurs-Parasites-Environnement dans les Maladies Tropicales Négligées Dues aux Trypanosomatides, 34398 Montpellier, France; [d]Institut Sénégalais de Recherches Agricoles, Laboratoire National d'Elevage et de Recherches Vétérinaires, Service de Parasitologie, BP 2057 Dakar, Senegal; [e]West African Science Service in Climate Change and Adapted Land Use, Climate Change Economics Research Program, Cheikh Anta Diop University, BP 5683, Dakar, Senegal; [f]Food and Agriculture Organization of the United Nations, Sub-Regional Office for Eastern Africa, P.O. Box 5536, Addis Ababa, Ethiopia; [g]Institut de Recherche pour le Développement, Unité Mixte de Recherche Interactions Hôtes-Vecteurs-Parasites-Environnement dans les Maladies Tropicales Négligées Dues aux Trypanosomatides, 34398 Montpellier, France; [h]Unité de Recherche Animal et Gestion Intégrée de Risques, Centre de Coopération Internationale en Recherche Agronomique pour le Développement, 34398 Montpellier, France; [i]Department Environment and Societies, University of Zimbabwe, Harare, Zimbabwe; [j]Insect Pest Control Laboratory, Joint Food and Agriculture Organization of the United Nations/International Atomic Energy Agency Programme of Nuclear Techniques in Food and Agriculture, A-1400 Vienna, Austria; and [k]Centre International de Recherche-Développement sur l'Elevage en Zone Sub-humide, B.P. 454, Bobo-Dioulasso, Burkina Faso

Tsetse flies are the cyclical vectors of deadly human and animal trypanosomes in sub-Saharan Africa. Tsetse control is a key component for the integrated management of both plagues, but local eradication successes have been limited to less than 2% of the infested area. This is attributed to either resurgence of residual populations that were omitted from the eradication campaign or reinvasion from neighboring infested areas. Here we focused on *Glossina palpalis gambiensis*, a riverine tsetse species representing the main vector of trypanosomoses in West Africa. We mapped landscape resistance to tsetse genetic flow, hereafter referred to as friction, to identify natural barriers that isolate tsetse populations. For this purpose, we fitted a statistical model of the genetic distance between 37 tsetse populations sampled in the region, using a set of remotely sensed environmental data as predictors. The least-cost path between these populations was then estimated using the predicted friction map. The method enabled us to avoid the subjectivity inherent in the expert-based weighting of environmental parameters. Finally, we identified potentially isolated clusters of *G. p. gambiensis* habitat based on a species distribution model and ranked them according to their predicted genetic distance to the main tsetse population. The methodology presented here will inform the choice on the most appropriate intervention strategies to be implemented against tsetse flies in different parts of Africa. It can also be used to control other pests and to support conservation of endangered species.

area-wide integrated pest management | eradication | vector control | remote sensing | resistance surface

Tsetse flies transmit trypanosomes, the causative agents of sleeping sickness (human African trypanosomosis, HAT) and nagana (African animal trypanosomosis, AAT). Through increased disease surveillance and treatment, the number of HAT cases has substantially declined in the last 15 y (1). However, the elimination of HAT as a public health problem also requires effective vector management (1). AAT continues to represent the greatest animal-health constraint to improved livestock production in sub-Saharan Africa, causing enormous economic losses (e.g., milk and meat production) (2). AAT also constrains the integration of crop farming and livestock keeping, a crucial component for the development of sustainable agricultural systems (3). Indeed, AAT affects animal draft power, and consequently crop production. Also, keeping less productive trypanotolerant cattle breeds pushes farmers to increase herd sizes with such negative environmental impacts as overgrazing. As an example, in the Niayes area of Senegal, it was estimated that the eradication of tsetse flies would allow cattle sales to triple whereas herd sizes would decrease by 45% (4).

The Challenges of Tsetse Elimination

Despite substantial efforts for over a century, deliberate efforts to reduce the vast tsetse belt have had very limited success (5). In past decades, spraying of residual insecticides was effective in certain areas, but this technique is no longer acceptable on environmental grounds. More recently, two environmentally friendly campaigns achieved sustained elimination by targeting isolated tsetse populations as a whole (6, 7). It is therefore useful to identify islands (8) or ecological islands (9) where isolated tsetse populations could be eradicated without risk of reinvasion. Although attempts have been made to identify isolated tsetse populations* (10, 11), a well-defined and reproducible method that can be applied on a regional scale is still lacking.

Landscape Friction, Genetics, and Dispersal

Given the high costs of field sampling, and the difficulty in accessing some of the sites, it is impossible to adopt a population genomic approach based on a systematic sampling of tsetse populations. Modeling landscape friction would thus represent a major advance

Significance

Tsetse flies transmit human and animal trypanosomoses in Africa, respectively a neglected disease (sleeping sickness) and the most important constraint to cattle production in infested countries (nagana), and they are the target of the Pan African Tsetse and Trypanosomoses Eradication Campaign (PATTEC). Here, we used genetic distances and remotely sensed environmental data to identify natural barriers to tsetse dispersal and potentially isolated tsetse populations for targeting elimination programs. The method can be used to prioritize intervention areas within the PATTEC initiative and it is applicable to the control campaigns of other vector and pest species, as well as to the conservation of endangered species in fragmented habitats.

to inform the prioritizing of tsetse elimination campaigns, with promising applications at the continent level.

Landscape friction, or its inverse, landscape permeability, modulates how animal species can move in the environment. In the field of landscape genetics, friction is modeled to (*i*) identify landscape and environmental features that constrain genetic connectivity, (*ii*) elucidate the ecological processes that influence spatial genetic structure, mainly to inform resources management and conservation, and (*iii*) predict how future landscape changes might influence genetic connectivity (12). Landscape friction has been studied in a number of species, with insects only represented in fewer than 10% of the studies (13). For example, studying friction allowed researchers to demonstrate that the rate of water loss plays a key role in the movement of a terrestrial woodland salamander, but also that models of habitat suitability or abundance may not be adequate proxies for gene flow (14).

In tsetse, consistent estimates of *Glossina palpalis gambiensis* dispersal at the microscale were obtained using direct methods (mark–release–recapture) as well as indirect ones (genetic isolation by distance) (15). Although a strong isolation by distance was observed in this species, tsetse populations separated by only 15 km of rice plantations (16) were found to be more isolated than others separated by 100 km of gallery forest (15). In other words, for this riverine tsetse species the friction of riparian woody vegetation is significantly lower than that of rice plantations. Despite its potential usefulness, no friction map is available for tsetse flies at any scale, and our attempts to generate one for *G. p. gambiensis* by using global land-cover maps and expert-based cost parameters (13) proved ineffective. By contrast, we built a friction map by iterating linear regression models of genetic distance and environmental parameters and by determining least-cost dispersal paths. The novelty of our approach is to relax the need for expert opinion and to rely fully on the genetic distance for an evidence-based mapping of landscape connectivity and for the identification of the most likely dispersal paths. We subsequently combined the genetics-based analysis of friction with a tsetse distribution model built using a fully different dataset, thus considering that habitat suitability and connectivity might not be influenced by the same environmental factors (14). The end result is a reproducible methodology that enabled us to locate potentially isolated tsetse populations that might be considered as targets in eradication programs.

Results and Discussion

Effect of Environmental Factors on Genetic Distance. Using a linear regression model, we estimated the relationship between genetic distance [Cavalli-Sforza and Edwards' chord distance (CSE), i.e., the response] and a set of environmental factors (the explanatory variables), the latter being initially calculated along the direct paths connecting tsetse populations pairwise (Figs. S1–S3). Expert-based permeability/friction scores had been first explored using global land-cover datasets (Global Land Cover 2000 and Globcover 2006). No significant correlation was found with genetic distance (Fig. S1, Table S1, and *Details on the Genetic Analysis*).

In the regression model, the main variables influencing genetic distance were (*i*) the geographic distance, (*ii*) being located within the same river basin, and (*iii*) three different metrics of habitat fragmentation, namely the patch density [number of habitat patches (i.e., tree cover >20%) within the 0.2° pixels where landscape friction is modeled], the class area [number of habitat pixels (500 × 500 m)]), and the maximum distance between habitat patches (Fig. 1). The findings were consistent with existing knowledge of *G. p. gambiensis* ecology. For example, isolation by distance is well known, as is the effect of watersheds on genetic distance, even if the latter does not lead to complete isolation (Fig. S4) (11). Human encroachment on tsetse habitat explains the positive effect of habitat fragmentation on genetic distance: The further apart the habitat patches, the more difficult for tsetse to disperse (Fig. 2) (17).

Identification of Tsetse Dispersal Paths. Direct lines connecting the sampled tsetse populations were initially used to model the genetic
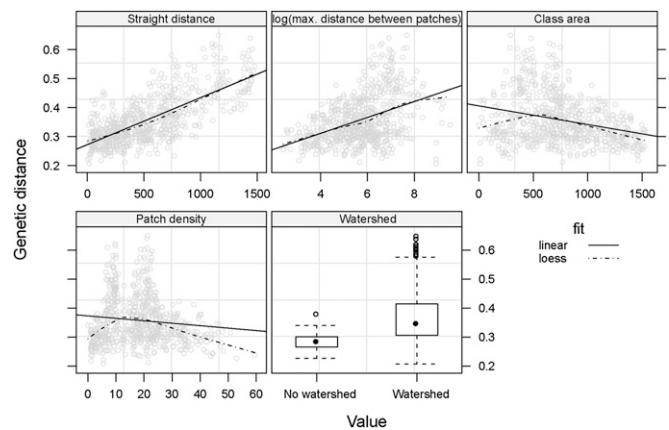

Fig. 1. Shape and amplitude of the relationships between genetic distance, great-circle distance and environmental variables. CSE was calculated between pairs of *G. p. gambiensis* populations (37 sampling sites listed in Table S1) and environmental variables are here extracted along the straight paths.

distance against the environmental variables, thereby generating the initial friction map. Subsequently, the average values for the environmental variables were recalculated along the least-cost paths based on the initial friction map (Fig. 3). To this end, a transition matrix was computed from the friction map. To define the connectedness between adjacent pixels, we used Rooks' distance as a neighborhood function, in which a given pixel is considered to be connected to the four adjacent pixels. Then, the least-cost paths between origin and destination points were calculated, minimizing the mean values of friction for the pixels crossed by the path. The new set of values of explanatory variables extracted along this least-cost path was used to refit the regression model. This procedure was repeated 20 times, and models fitted at each iteration were compared with the Akaike information criterion corrected for small sample size (AICc): The smaller, the better. A large reduction of AICc was observed between the initial model based on direct lines and the AICc-best model based on least-cost paths: Δ AICc = 18 (Fig. 3A). Thus, the regression model based on least-cost paths (seventh iteration) was much more plausible than the initial one. It also minimized the root mean squared error (Fig. 3B).

Apart from the time between sampling events and the geographical distance, all variables retained in the AICc-best model (coefficients in Table S2) were describing landscape connectivity (i.e., landscape fragmentation metrics and the presence of a watershed) (Fig. 2). There was a nonlinear relationship between the density and area of habitat patches, as expected in a fragmentation process (Fig. S5). Moreover, the interaction term between these two variables was retained in the final model. The variables informing on the composition and shape of the fragmented landscape and the geographic distance became more important in the final model, whereas the importance of watersheds and interactions was reduced (Fig. S6).

The use of least-cost distance confirmed the significant impact of time between sampling dates on the genetic distance (Table S2) (16). More importantly, it revealed the importance of landscape features related to functional connectivity (Table S2). The iterative, least-cost-based analysis also improved the mapping of ecological barriers to tsetse dispersal, with a more contrasted picture of friction (Fig. 3C).

Distribution of *G. p. gambiensis* in the Study Area and Combination with Landscape Friction. The habitat suitability for *G. p. gambiensis* was estimated using a maximum entropy (MaxEnt) model and mapped independently from landscape friction. Tsetse habitat was positively associated to vegetation activity [i.e., normalized difference vegetation index (NDVI)], average precipitations, and humidity. Conversely, high values for temperature-related variables
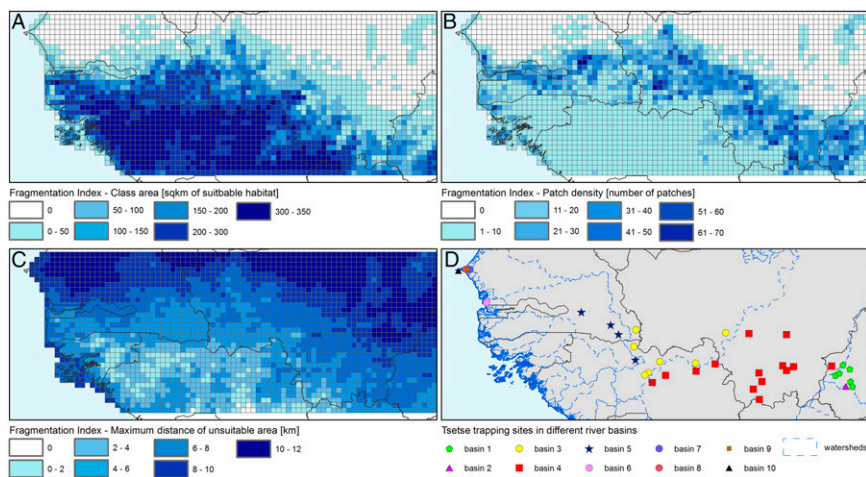
Fig. 2. Landscape fragmentation and river basins. Landscape fragmentation of *G. p. gambiensis* habitat based on a tree cover threshold of 20% (year 2000) (44) and related linear fragmentation indices. (*A*) Patch area. (*B*) Patch density. (*C*) Maximum distance of unsuitable area (or maximum distance between patches). (*D*) Locations of the tsetse sampling sites grouped by river basin (45).

[land surface temperature (LST) and air temperature] led to a low suitability index. Fig. 4 presents the respective contributions and response curves for the different variables, the most important being maximum LST and average precipitation. The predictive power of the MaxEnt model was high, with an area under the curve of 0.84 (Fig. 4). Moreover, the precision of MaxEnt predictions was the highest in the areas of interest (northern limit of the tsetse belt), which was also the most intensively sampled area (Fig. S7). Finally, we used a density-based clustering algorithm applied to the MaxEnt output to identify eight clusters of suitable habitat located at least 10 km apart from the main tsetse habitat.

Model Predictions and Consequences for Tsetse Control. Fig. 5 presents the eight potentially isolated clusters of tsetse habitat located at the northern distribution limit of the *G. p. gambiensis* belt in West Africa. The population with the highest predicted genetic distance from the main tsetse belt ($P = 0.003$) was close to Thiès (Senegal). It is also the target of an ongoing eradication campaign. For this population, genetic isolation was confirmed by independent morphometric and genetic studies (9). Two other clusters (6 and 8) with similar genetic distances from the tsetse belt seemed to be isolated ($P = 0.001$) and therefore represent interesting potential targets for elimination efforts. Finally, two other clusters could be isolated (2 and 7, $P < 0.05$). Interestingly, the situation in cluster 2 (Bijagos Islands in Guinea Bissau) is reminiscent of the Loos Islands in Guinea (not visible in Fig. 5). The tsetse populations in the Loos Islands were recently targeted by an elimination program following the demonstration of their isolation (8).

The present study provides information on potential targets for tsetse elimination across a vast area. However, should one of these populations be selected for an elimination program, more comprehensive local studies would be needed, both to characterize the exact extent and connectivity of the infested area and to confirm its genetic isolation. These studies should include systematic sampling of suitable habitats (18) and an independent genetic analysis involving the target population and those closest to it (9).

Future Prospects. Microsatellite genetic markers are available for the most important tsetse species: *Glossina fuscipes*, *Glossina morsitans*, *Glossina pallidipes*, and *Glossina tachinoides*. Furthermore, the recent sequencing of the full genome of *G. morsitans* offers new prospects for either additional microsatellite markers or other markers such as single-nucleotide polymorphisms (19). Applying the methodology described in this study to other tsetse species and regions would provide decision makers with crucial information on where control or eradication programs might be

more appropriate. Friction maps might also help in those situations where the populations targeted for eradication are not isolated (e.g., the Mouhoun River in Burkina Faso and northwestern Ghana). In fact, artificial barriers to reinvasion such as traps impregnated with insecticides (6) would be more effective if deployed
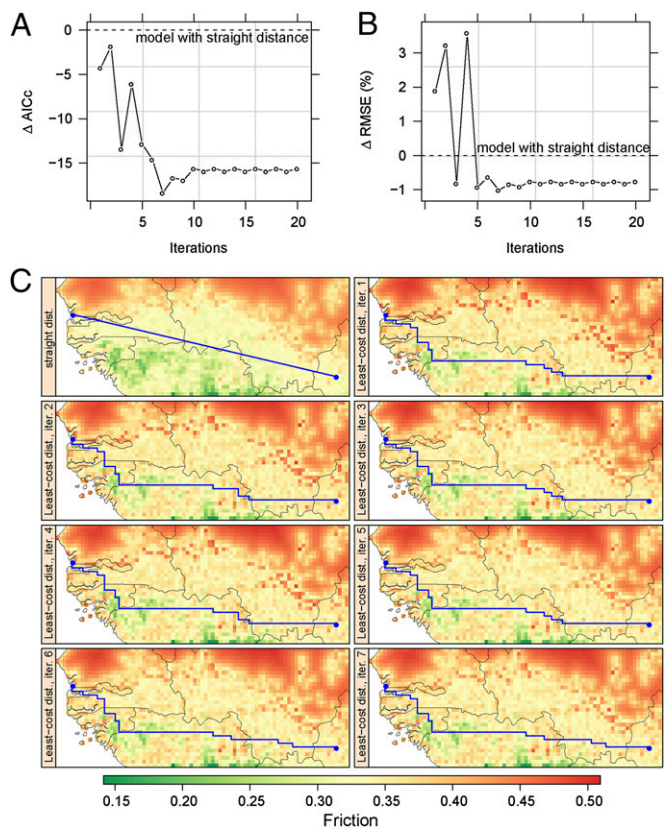

Fig. 3. Least-cost distance vs. straight distance. (*A*) Observed changes in Akaike information criterion with small-sample size correction (AICc) and (*B*) rmse when replacing straight distance with least-cost distance computed from the friction raster, and iterating the process (*x* axis). (*C*) Changes in landscape genetic friction (colored map) and in least-cost distance (blue line) between two tsetse populations over the first seven iterations.
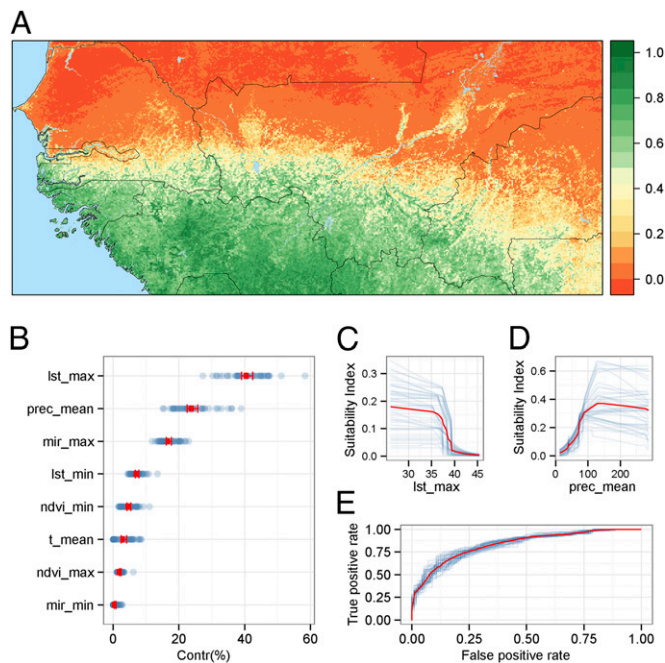
APPLIED BIOLOGICAL SCIENCES

Fig. 4. Distribution of *G. p. gambiensis* in West Africa. (*A*) Mean habitat suitability index predicted by a MaxEnt model. The index varies between 0 (less suitable, red scale) and 1 (highly suitable, green scale). (*B*) Contribution of variables to the suitability index by decreasing importance (95% confidence interval in red and individual values in blue). lst_max, maximum land surface temperature (MODIS); lst_min, minimum land surface temperature (MODIS); mir_max, maximum mid-infrared reflectance (MODIS); mir_min, minimum mid-infrared reflectance; ndvi_max, maximum normalized difference vegetation index (MODIS); ndvi_min, minimum normalized difference vegetation index (MODIS); prec_mean, mean yearly rainfalls (WorldClim grid); t_mean, mean annual temperature (WorldClim grid). (*C* and *D*) Response curves of the most contributing variables (lst_max and prec_mean, respectively). (*E*) Area under the curve for the average MaxEnt model (in red) and the 45 submodels (in blue) (see *Details on the MaxEnt Model* for details).

in high-friction areas. The use of such artificial barriers might therefore enable sequential eradication programs, by dividing the target populations into partially isolated subunits (20). Furthermore, in those areas exposed to strong reinvasion pressure, landscape friction analysis could guide the adoption of alternative strategies (e.g., reduction of tsetse densities below the threshold of disease transmission), thus preventing major economic losses due to unsuccessful eradication attempts.

Finally, identifying natural barriers to dispersal and quantifying their environmental determinants might help to manage other pests, or conversely it could be used to improve the conservation of endangered species occurring as metapopulations (21). Indeed, locating genetic corridors across high-friction landscapes is becoming crucial for the conservation of natural populations in a context of increasing fragmentation of ecosystems (12).

Methods

Genetic Analysis. We inferred tsetse dispersal using the CSE calculated between 37 populations of *G. p. gambiensis* from West Africa. Samples were collected along the northern limit of the distribution, where tsetse habitat is most fragmented (22) (Table S3). Most populations (24 out of 37) were specifically sampled for this study using biconical traps (1–11 traps by site). Traps were set at ~100-m intervals for a maximum period of 1 wk and with a maximum distance of 1 km between first and last traps (10). We also included in the analysis 13 previously sampled populations (9, 10). The geographical coordinates and data collection dates are presented in Table S3. Each population was sampled once.

In total, 1,158 flies were genotyped at seven loci following a previously described protocol (16). All genotyping was handled or supervised by the same person (S.R.), thus ensuring optimal calibration of allele sizes across

subsamples. Males were coded as homozygous at X-linked loci. Overall, 61% of the flies were females, which are more informative given that four out of the seven loci are X-linked. Details on the genotyping procedure and the loci selected are presented in *Details on the Genetic Analysis*, together with tests of linkage disequilibrium and departure from Hardy–Weinberg (HW) equilibrium.

Three different genetic distances were initially explored: Wright's fixation index F_{ST} (23), CSE (24), and Bowcock et al.'s shared allelic distance (25). After an exploratory data analysis, CSE was selected, because it behaves better in case of missing data and is more appropriate for measuring relative distances between pairs of populations (26–28). We detail how CSE was calculated in *Details on the Genetic Analysis*.

Environmental Datasets for the Analysis of Genetic Distance. First, we explored the relationship between CSE and expert-based land-cover permeability scores (Table S1 and Fig. S1). Because of the failure of the latter to predict observed genetic distances, a range of spatially explicit environmental datasets selected based on the ecology of *G. p. gambiensis* were explored as explanatory variables. We considered climate (temperature and rainfall), land cover, human and cattle population, and topography (average slope and elevation change) (Figs. S2 and S3 and *Environmental Variables and Relationship with the Genetic Distance*). We also considered hydrological features (river basins) and habitat fragmentation metrics derived from Moderate Resolution Imaging Spectroradiometer (MODIS) tree cover (i.e., the area and density of patches of suitable habitat and the maximum distance between patches of suitable habitat) (Fig. 2, Fig. S4, and *Environmental Variables and Relationship with the Genetic Distance*). Considering the collection dates of the entomological data (2007–2010), and given the studied genetic markers, we focused on environmental datasets collected after 2000. For all gridded environmental datasets, average values were calculated along each line connecting tsetse sampling sites pairwise. Principal
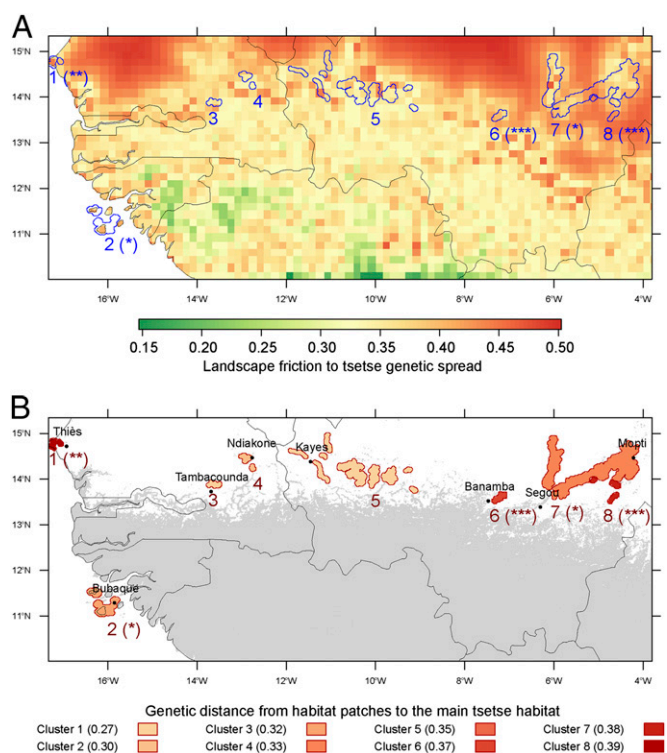

Fig. 5. Isolated patches of suitable habitat for *G. p. gambiensis*. (*A*) Landscape friction is the colored background, and habitat patches are delimited with blue contours. (*B*) The main tsetse belt predicted by MaxEnt for a sensitivity of 0.90 is in gray and habitat patches are shown as filled, red shapes. Contours and shapes of isolated patches were defined as 5-km radius buffers around pixels of habitat patches. The genetic distance of these patches to the main tsetse belt (reddish scale) was predicted by the AICc-best regression model along least-cost paths. Asterisks after cluster numbers represent the P values for the friction between the patches and the general habitat: (***) $P = 10^{-3}$, (**) $10^{-3} \leq P < 10^{-2}$, (*) $10^{-2} \leq P < 5 \cdot 10^{-2}$.

Bouyer et al.

components analysis was used to identify the most correlated variables. When strong correlations were found ($|r| > 0.8$), one of the variables was discarded, and the one with the most straightforward or acknowledged effect on the genetic distance was retained (*Environmental Variables and Relationship with the Genetic Distance*). To assess the shape and strength of the relationship between genetic distance and predictors, scatterplots were drawn with superimposed linear and loess-smoothed fits (Fig. 1 and Fig. S4). To account for the nonlinear fragmentation process (Fig. S5), the patch density was discretized into three categories (low, medium, and high). Additional data on this exploration phase and on how the data were prepared for the model are presented in *Environmental Variables and Relationship with the Genetic Distance*.

Linear Regression Model of the Genetic Distance. The goal was to find the best environmental predictors of the genetic distance between pairs of tsetse fly populations. We used a linear regression model fitted with generalized least squares (GLS) (29), having the genetic distance (CSE) as the response, and the selected environmental variables as the predictors. The time elapsed between population sampling was forced into the models to control for possible genetic drift. To account for possible autocorrelation, we clustered tsetse populations according to the geographic distance. Hierarchical ascending clustering (Ward method) was used to form partitions of various sizes (from 1 to 19 clusters) based on the Euclidian distance between pairs of populations. Cluster membership was then used to define the grouping structure in the GLS model (30). We selected the eight-cluster partition for which AICc was the lowest with the full GLS model (with all fixed effects) (31). Preliminary analyses revealed that model residuals increased with the fitted genetic distance. To account for this heteroscedasticity, we modeled residuals variance with a power function of the fitted values. Model goodness of fit was assessed using various indicators, including the proportion of variance explained by the fixed effects, quantile–quantile plots of residuals, and the detection of influential observations for GLS coefficients.

Finally, we selected the AICc-best model among all possible submodels in which were forced the Euclidian distance between tsetse populations and the time elapsed between population sampling. Regarding model validation, model selection with Akaike information criteria is formally equivalent to model cross-validation (32). We checked our results with the asymptotically equivalent leave-one-cluster-out cross-validation (CLCV). To do so, we fitted the model to the data with all of the cluster-based groups of distances but one, and predicted the genetic distance with this model for the populations belonging to the left-out group. Prediction errors were then summed for this group, and the process was iterated for all groups. The averaged prediction error was then used as the CLCV indicator to compare the 10 AICc-best models. The first four models were very close in terms of AICc and CLCV, and more generally there was a good agreement between AICc and CLCV (Spearman's rank correlation of 0.65, $P = 0.02$).

To build the friction maps, the AICc-best model was used to predict the genetic distance at each pixel location for the different predictors, setting at 0 both the time elapsed between population sampling and the geographical distance.

Building the Least-Cost Paths. The first iteration of the least-cost paths was based on the initial friction map, as built using the direct paths. Least-cost distances between origin and destination points were calculated using the functions available in the raster and gdistance packages for R (33, 34). Then, averages for all environmental variables were recalculated along the least-cost paths, and Euclidian distances were replaced by the least-cost distances. We subsequently refitted the full model and we selected the AICc-best submodel. The latter was then used to predict the friction across the study region. Finally, we recomputed the least-cost distances based on the updated friction map and iterated this process until the AICc of the best model was stabilized (Fig. 3A). Fig. 3C presents the initial friction and its changes for the first seven iterations. Table S2 and Fig. S6 present the coefficients of the AICc-best model used to build the final friction map and to predict the genetic distance between the potentially isolated tsetse populations associated with the eight habitat clusters (Fig. 5). The dataset including all environmental parameters and the genetic distances between pairs of populations is available as Dataset S1.

Tsetse Distribution Model. The entomological data used for the regional distribution model of *G. p. gambiensis* originated from recent baseline surveys for tsetse eradication projects in West Africa: 2007–2008 in Senegal (18), 2008–2009 in Ghana, and 2007–2012 in Burkina Faso (35). Unbaited biconical traps were used in all surveys (36). For the present analysis, only presence/absence

data were used. Absence data were filtered by the duration of trapping (≥3 d), and absence data within 5 km from a presence data were discarded. Presence and absence data were also filtered to keep only one presence or absence point within a radius of 5 km. From the initial 2,853 presence and 6,088 absence records, 450 and 516 data points, respectively, were finally retained.

Regarding environmental data used to predict habitat suitability, time series of high-spatial-resolution remote sensing data (1 km) were downloaded, cleaned, and summarized to build relevant environmental and climatic covariates. We combined 11 y of MODIS vegetation and thermal products (January 2003–December 2013). Eight-day composite daytime (DLST) and nighttime land surface temperature (NLST) were extracted from MOD11A2/MYD11A2 temperature and emissivity MODIS products. DLST and NLST were used as proxies for both soil and air temperature, which play an important role in shaping tsetse habitat. Low-quality pixels were removed from the raw data using the quality assessment layer and outliers were filtered using a variant of the boxplot algorithm (37). Vegetation indices at 1 km of spatial resolution and with temporal resolution of 16 d (MOD13A2/MYD13A2) were also downloaded and processed using the quality assessment layer. In particular, the NDVI and middle infrared (MIR) reflectance were selected to describe the vegetation and soil condition in the study area. Temperature and precipitation from WorldClim were also used (38).

A MaxEnt model was used to estimate a habitat suitability index for *G. p. gambiensis* in the study area (39). The logistic output from this method is a suitability index that ranges between 0 (less suitable habitat) and 1 (highly suitable habitat). The threshold for presence was set to allow a 90% sensitivity (40). Details on the parameterization of MaxEnt and the selection of pseudoabsences are available in *Details on the MaxEnt Model*.

Identification of Isolated Patches. To identify the connected patches from the MaxEnt output, we used the function ConnCompLabel in the SDMTools package (41). Then, we used a clustering algorithm to detect clusters of pixels based on their geographical proximity. To this end, we used the function dbscan from the eponymous R package (42). We withdrew isolated pixels as well as those belonging to small clusters (fewer than 20 pixels). Then, we computed the minimum distance between the (centroids of) cluster pixels and those from the general population. We discarded clusters located at less than 10 km from the main tsetse belt because they were unlikely to be genetically isolated from it, and these pixels were thereafter considered as part of the main tsetse belt. Then, we grouped together clusters that were geographically close to each other using a hierarchical ascending classification procedure, with the so-called simple (neighbor-joining) algorithm. At the end of this step, nine clusters were left. One of them was discarded because it was cut by the eastern limit of the analysis window. Finally, we computed the predicted least-cost distance between the clusters and the main tsetse belt using the AICc-best model and the friction raster formerly estimated (Fig. 5 and Table S2). In this sample of eight habitat patches, the correlation of geographic and genetic distances was not significant (Spearman's rank correlation of 0.43, $P = 0.30$). To test the significance of the isolation of these clusters, a statistical test was built whereby for each cluster the genetic distance to the main tsetse belt was compared with those between 999 pairs of points randomly generated within the main belt, with the same geographical distance between them as between the patch and the general population (minimum $P = 0.001$). All genetic distances between pairs of points were computed with the procedure previously described, using the AICc-best model and the friction raster formerly estimated. All analyses were conducted using R software (43).

1. WHO (2013) *Control and Surveillance of Human African Trypanosomiasis* (World Health Organization, Geneva).
2. Swallow BM, ed (2000) *Impacts of Trypanosomiasis on African Agriculture* (FAO, Rome).
3. Alsan M (2015) The effect of the tsetse fly on African development. *Am Econ Rev* 105(1):382–410.
4. Bouyer F, et al. (2014) Ex-ante benefit-cost analysis of the elimination of a Glossina palpalis gambiensis population in the Niayes of Senegal. *PLoS Negl Trop Dis* 8(8):e3112.
5. Vreysen MJB, Seck MT, Sall B, Bouyer J (2013) Tsetse flies: Their biology and control using area-wide integrated pest management approaches. *J Invertebr Pathol* 112(Suppl):S15–S25.
6. Kgori PM, Modo S, Torr SJ (2006) The use of aerial spraying to eliminate tsetse from the Okavango Delta of Botswana. *Acta Trop* 99(2-3):184–199.
7. Vreysen MJB, et al. (2000) *Glossina austeni* (Diptera: Glossinidae) eradicated on the island of Unguja, Zanzibar, using the sterile insect technique. *J Econ Entomol* 93(1):123–135.
8. Solano P, et al. (2009) The population structure of *Glossina palpalis gambiensis* from island and continental locations in Coastal Guinea. *PLoS Negl Trop Dis* 3(3):e392.
9. Solano P, et al. (2010) Population genetics as a tool to select tsetse control strategies: Suppression or eradication of Glossina palpalis gambiensis in the Niayes of Senegal. *PLoS Negl Trop Dis* 4(5):e692.
10. Koné N, et al. (2011) Contrasting population structures of two vectors of African trypanosomoses in Burkina Faso: Consequences for control. *PLoS Negl Trop Dis* 5(6):e1217.
11. Vreysen MJ, et al. (2013) Release-recapture studies confirm dispersal of *Glossina palpalis gambiensis* between river basins in Mali. *PLoS Negl Trop Dis* 7(4):e2022.
12. Spear SF, Balkenhol N, Fortin M-J, McRae BH, Scribner K (2010) Use of resistance surfaces for landscape genetic studies: Considerations for parameterization and analysis. *Mol Ecol* 19(17):3576–3591.
13. Zeller KA, McGarigal K, Whiteley AR (2012) Estimating landscape resistance to movement: A review. *Landscape Ecol* 27(6):777–797.
14. Peterman WE, Connette GM, Semlitsch RD, Eggert LS (2014) Ecological resistance surfaces predict fine-scale genetic differentiation in a terrestrial woodland salamander. *Mol Ecol* 23(10):2402–2413.
15. Bouyer J, et al. (2009) Population sizes and dispersal pattern of tsetse flies: Rolling on the river? *Mol Ecol* 18(13):2787–2797.
16. De Meeûs T, Ravel S, Rayaisse J-B, Courtin F, Solano P (2012) Understanding local population genetics of tsetse: The case of an isolated population of *Glossina palpalis gambiensis* in Burkina Faso. *Infect Genet Evol* 12(6):1229–1234.
17. Dicko AH, et al. (2014) Using species distribution models to optimize vector control in the framework of the tsetse eradication campaign in Senegal. *Proc Natl Acad Sci USA* 111(28):10149–10154.
18. Bouyer J, Seck MT, Sall B, Guerrini L, Vreysen MJB (2010) Stratified entomological sampling in preparation of an area-wide integrated pest management programme: The example of *Glossina palpalis gambiensis* in the Niayes of Senegal. *J Med Entomol* 47(4):543–552.
19. International Glossina Genome Initiative (2014) Genome sequence of the tsetse fly (*Glossina morsitans*): Vector of African trypanosomiasis. *Science* 344(6182):380–386.
20. Hendrichs J, Vreysen MJB, Enkerlin WR, Cayol JP (2005) Strategic options in using sterile insects for area-wide integrated pest management. *Sterile Insect Technique*, eds Dyck VA, Hendrichs J, Robinson AS (Springer, Dordrecht, The Netherlands), pp 563–600.
21. Hanski I, Ovaskainen O (2000) The metapopulation capacity of a fragmented landscape. *Nature* 404(6779):755–758.
22. Guerrini L, Bord JP, Ducheyne E, Bouyer J (2008) Fragmentation analysis for prediction of suitable habitat for vectors: Example of riverine tsetse flies in Burkina Faso. *J Med Entomol* 45(6):1180–1186.
23. Wright S (1965) The interpretation of population structure by F-statistics with special regard to system of mating. *Evolution* 19(3):395–420.
24. Cavalli-Sforza LL, Edwards AWF (1967) Phylogenetic analysis. Models and estimation procedures. *Am J Hum Genet* 19(3 Pt 1):233–257.
25. Bowcock AM, et al. (1994) High resolution of human evolutionary trees with polymorphic microsatellites. *Nature* 368(6470):455–457.
26. de Meeûs T, et al. (2007) Population genetics and molecular epidemiology or how to "débusquer la bête". *Infect Genet Evol* 7(2):308–332.
27. Takezaki N, Nei M (1996) Genetic distances and reconstruction of phylogenetic trees from microsatellite DNA. *Genetics* 144(1):389–399.
28. Kalinowski ST (2002) Evolutionary and statistical properties of three genetic distances. *Mol Ecol* 11(8):1263–1273.
29. Laird NM, Ware JH (1982) Random-effects models for longitudinal data. *Biometrics* 38(4):963–974.
30. Dormann CF, et al. (2007) Methods to account for spatial autocorrelation in the analysis of species distributional data: A review. *Ecography* 30(5):609–628.
31. Hurvich CM, Tsai C-L (1995) Model selection for extended quasi-likelihood models in small samples. *Biometrics* 51(3):1077–1084.
32. Fang Y (2011) Asymptotic equivalence between cross-validations and Akaike Information Criteria in mixed-effects models. *J Data Sci* 9:15–21.
33. Hijmans RJ (2015) raster: Geographic data analysis and modeling, R package version 2.4-15. Available at https://cran.r-project.org/web/packages/raster/index.html.
34. van Etten J (2012) gdistance: Distances and routes on geographical grids, R package version 1:1-4. Available at CRAN.R-project.org/package=gdistance.
35. Dicko AH, et al. (2015) A spatio-temporal model of African animal trypanosomosis risk. *PLoS Negl Trop Dis* 9(7):e0003921.
36. Challier A, Laveissière C (1973) Un nouveau piège pour la capture des glossines (*Glossina*: Diptera, Muscidae): Description et essais sur le terrain. *Cah ORSTOM sér Ent Méd Parasitol* 10(4):251–262.
37. Neteler M (2010) Estimating daily land surface temperatures in mountainous environments by reconstructed MODIS LST data. *Remote Sens* 2(1):333–351.
38. Hijmans R, Cameron S, Parra J, Jones P, Jarvis A (2005) Very high resolution interpolated climate surfaces for global land areas. *Int J Climatol* 25:1965–1978.
39. Elith J, et al. (2011) A statistical explanation of MaxEnt for ecologists. *Divers Distrib* 17(1):43–57.
40. Liu C, Berry PM, Dawson TP, Pearson RG (2005) Selecting thresholds of occurrence in the prediction of species distributions. *Ecography* 28(3):385–393.
41. VanDerWal J, Falconi L, Januchowski S, Shoo L, Storlie C (2014) SDMTools: Species distribution modelling tools: Tools for processing data associated with species distribution modelling exercises, R package version 1.1-221. Available at https://cran.r-project.org/web/packages/SDMTools/index.html.
42. Hahsler M (2015) dbscan: Density Based Clustering of Applications with Noise (DBSCAN), R package version 0.9-1. Available at https://cran.r-project.org/web/packages/dbscan/index.html.
43. R Core Team (2015) R: A language and environment for statistical computing (R Foundation for Statistical Computing, Vienna). Available at www.R-project.org.
44. Hansen M, et al. (2003) Global percent tree cover at a spatial resolution of 500 meters: First results of the MODIS vegetation continuous fields algorithm. *Earth Interact* 7(10):1–15.
45. Lehner B, Verdin K, Jarvis A (2008) New global hydrography derived from spaceborne elevation data. *Eos* 89(10):93–94.
46. Solano P, Duvallet G, Dumas V, Cuisance D, Cuny G (1997) Microsatellite markers for genetic population studies in *Glossina palpalis* (Diptera: Glossinidae). *Acta Trop* 65(3):175–180.
47. Luna C, et al. (2001) Microsatellite polymorphism in tsetse flies (Diptera: Glossinidae). *J Med Entomol* 38(3):376–381.
48. Baker MD, Krafsur ES (2001) Identification and properties of microsatellite markers in tsetse flies *Glossina morsitans* sensu lato (Diptera: Glossinidae). *Mol Ecol Notes* 1(4):234–236.
49. De Meeûs T, Guégan JF, Teriokhin AT (2009) MultiTest V.1.2, a program to binomially combine independent tests and performance comparison with other related methods on proportional data. *BMC Bioinformatics* 10:443.
50. Goudet J (1995) FSTAT (v. 1.2): A computer program to calculate F-statistics. *J Hered* 86(6):485–486.
51. Van Oosterhout C, Hutchinson WF, Wills DPM, Shipley P (2004) MICRO-CHECKER: Software for identifying and correcting genotyping errors in microsatellite data. *Mol Ecol Notes* 4(3):535–538.
52. Brookfield JFY (1996) A simple new method for estimating null allele frequency from heterozygote deficiency. *Mol Ecol* 5(3):453–455.
53. Dieringer D, Schlötterer C (2003) Microsatellite analyser (MSA): A platform independent analysis tool for large microsatellite data sets. *Mol Ecol Notes* 3(1):167–169.
54. Coombs JA, Letcher BH, Nislow KH (2008) create: A software to create input files from diploid genotypic data for 52 genetic software programs. *Mol Ecol Resour* 8(3):578–580.
55. Mayaux P, Bartholomé E, Fritz S, Belward A (2004) A new land-cover map of Africa for the year 2000. *J Biogeogr* 31(6):861–877.
56. Arino O, et al. (2007) GlobCover: ESA service for global land cover from MERIS. *IEEE International Geoscience and Remote Sensing Symposium, 2007* (IEEE, New York), pp 2412–2415.
57. Van Zyl JJ (2001) The Shuttle Radar Topography Mission (SRTM): A breakthrough in remote sensing of topography. *Acta Astronaut* 48(5):559–565.
58. Keyghobadi N, Roland J, Strobeck C (1999) Influence of landscape on the population genetic structure of the alpine butterfly parnassius smintheus (Papilionidae). *Mol Ecol* 8(9):1481–1495.
59. Balk D, Yetman G (2004) *The Global Distribution of Population: Evaluating the Gains in Resolution Refinement* (Center for International Earth Science Information Network, Columbia Univ, New York).
60. Center for International Earth Science Information Network, Columbia University International Food Policy Research Institute, the World Bank, and Centro Internacional de Agricultura Tropical (2004) *Global Rural-Urban Mapping Project (GRUMP): Urban/Rural Population Grids* (Center for International Earth Science Information Network, Columbia Univ, Palisades, NY).
61. Dobson J, Bright E, Coleman P, Durfee R, Worley B (2000) LandScan: A global population database for estimating populations at risk. *Photogramm Eng Remote Sensing* 66(7):849–857.
62. Wint W, Robinson TP (2007) *Gridded Livestock of the World 2007* (FAO, Rome).
63. Dudík M, Phillips SJ, Schapire RE (2005) Correcting sample selection bias in maximum entropy density estimation. *Advances in Neural Information Processing Systems* (MIT Press, Cambridge, MA), pp 323–330.
64. Phillips SJ, et al. (2009) Sample selection bias and presence-only distribution models: Implications for background and pseudo-absence data. *Ecol Appl* 19(1):181–197.
65. Zomer RJ, Trabucco A, Bossio DA, Verchot LV (2008) Climate change mitigation: A spatial analysis of global land suitability for clean development mechanism afforestation and reforestation. *Agric Ecosyst Environ* 126(1):67–80.